

Far field observation and theoretical analyses of light directional imaging in metamaterial with stacked metal-dielectric films

Changtao Wang, Ping Gao, Xing Tao, Zeyu Zhao, Mingbo Pu, Po Chen, and Xiangang Luo

Citation: [Applied Physics Letters](#) **103**, 031911 (2013); doi: 10.1063/1.4815924

View online: <http://dx.doi.org/10.1063/1.4815924>

View Table of Contents: <http://scitation.aip.org/content/aip/journal/apl/103/3?ver=pdfcov>

Published by the [AIP Publishing](#)

Articles you may be interested in

[Improved transmittance in metal-dielectric metamaterials using diffraction grating](#)

Appl. Phys. Lett. **104**, 171904 (2014); 10.1063/1.4875555

[Geometrical parameters controlled focusing and enhancing near field in infinite circular metal-dielectric multilayered cylinder](#)

Appl. Phys. Lett. **102**, 123107 (2013); 10.1063/1.4798662

[Direct observation of amplified spontaneous emission of surface plasmon polaritons at metal/dielectric interfaces](#)

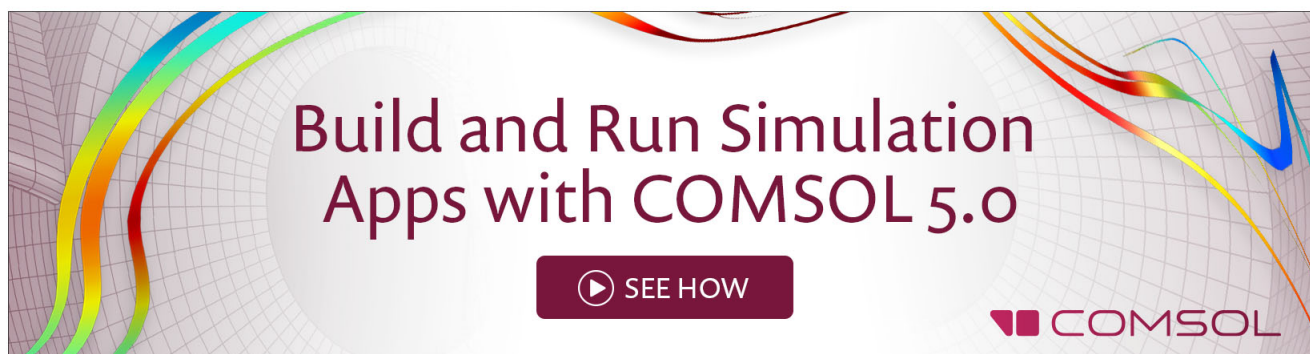
Appl. Phys. Lett. **98**, 261912 (2011); 10.1063/1.3605599

[Enhanced transmittance and fields of a thick metal sandwiched between two dielectric photonic crystals](#)

J. Appl. Phys. **108**, 103111 (2010); 10.1063/1.3512903

[Polarization beam splitting through an anisotropic metamaterial slab realized by a layered metal-dielectric structure](#)

Appl. Phys. Lett. **92**, 071114 (2008); 10.1063/1.2884322

A promotional banner for COMSOL 5.0. It features a background of colorful, flowing lines in shades of blue, green, yellow, and red, set against a light gray grid. The text 'Build and Run Simulation Apps with COMSOL 5.0' is prominently displayed in a dark red font. Below the text is a dark red button with a white play icon and the text 'SEE HOW'. The COMSOL logo is in the bottom right corner.

Far field observation and theoretical analyses of light directional imaging in metamaterial with stacked metal-dielectric films

Changtao Wang,¹ Ping Gao,¹ Xing Tao,¹ Zeyu Zhao,¹ Mingbo Pu,¹ Po Chen,² and Xiangang Luo^{1,a)}

¹State Key Laboratory of Optical Technologies on Nano-Fabrication and Micro-Engineering, Institute of Optics and Electronics, Chinese Academy of Sciences, P.O. Box 350, Chengdu 610209, China

²Department of Geology and Geophysics, University of Wyoming, Laramie, Wyoming 82071, USA

(Received 24 March 2013; accepted 29 June 2013; published online 17 July 2013)

We report experimental observation of directional imaging of evanescent waves in layered metal-dielectric metamaterial. The investigation is performed with Ag/SiO₂ multilayers combined with nano-object featured by a silicon mask slit. Evanescent waves of directional imaging are transferred to far field by roughening the top Ag layer and observed with a microscope objective. Experimental results agree well with numerical simulations. In addition, directional imaging behavior dependences on geometrical parameters are further presented and show great deviations with effective medium theory in some cases. © 2013 AIP Publishing LLC. [<http://dx.doi.org/10.1063/1.4815924>]

The exponential decay of the evanescent waves carrying sub-wavelength information leads to the physical limitation on the maximum achievable resolution of conventional optical systems. Recently, alternatively stacked metal and dielectric layers (ASMDLs) were proposed as a specific type of metamaterial to overcome the diffraction limit.^{1,2} It is predicated numerically and analytically that the extraordinary directional propagation of evanescent waves in the metamaterial is due to the hyperbolic dispersion relation of the metamaterial in which most energy of evanescent waves propagate perpendicularly to the asymptote line. In Ref. 2, this behavior is viewed as directional imaging ability from one side to the other side of metamaterial slab. In general, the evanescent waves of the opposite sign of transversal wave vector k_x propagate in two directions, thus form two or more images on the output plane due to multiple reflection behavior inside metamaterial structure. This process could be viewed as the coupling of evanescent wave modes in the manner of coupled surface plasmons (SPs) between the adjacent metal-dielectric interfaces. Specially, when the permittivity of metal and dielectric films match like superlens,³⁻⁵ the waves propagate perpendicularly to layers, thus only one image forms. The directional imaging property provides the generalized basis for a number of imaging methods utilizing stacked metal dielectric films, including the superlens in multi layers form,^{6,7} hyperlens,⁸⁻¹⁰ subwavelength imaging in a canalization way¹¹ and by combining negative and positive refraction systems,¹² etc.

In this paper, we report the experimental observation of light directional imaging in the ASMDL metamaterial consisting of Ag/SiO₂ multilayers with nano-objects featured by a silicon mask slit on one side. Instead of measuring surface plasmon behaviors by photoresist or near-field scanning methods, we utilize surface roughness to convert surface plasmon waves to propagating waves and subsequently being detected and imaged in the far field. The control experiments and numerical simulations provide clear evidences of the

observed directional imaging in the ASMDL metamaterial. In addition, further investigation shows that directional imaging behavior usually deviates greatly with that predicted by effective media theory (EMT), indicating the necessity of rigorous coupled wave analysis (RCWA) in investigating these behaviors.

The schematic diagram of the ASMDL metamaterial employed in the experiment is shown in Fig. 1. The metamaterial is composed by alternatively stacking 8 layers of Ag and 7 layers of SiO₂ films, and each layer is 20 nm thick. On the one side of films is an 80 nm wide slit aperture on the substrate and spaced by a Polymethyl Methacrylate (PMMA) layer. A normal plane wave at wavelength of 532 nm in TM-polarization (magnetic field direction along the slit) illuminates from the bottom of the substrate. The relative permittivities for Ag and SiO₂ are $\epsilon_{Ag} = -11.784 + 0.3722i$ (Ref. 13) and $\epsilon_{SiO_2} = 2.13$ (Ref. 14) at 532 nm, respectively.

Shown in Fig. 2(a) is the simulation result performed by COMSOL MULTIPHYSICS 3.5. Obviously, surface plasmons are excited at the slit aperture exit and propagate in two directions and two light lines (images of slit aperture) separated by 1.59 μm are formed at the top layer, corresponding to about 68.2° light propagation direction inside metamaterial. Note normally evanescent waves are transmitted in the metamaterial, as indicated by the subwavelength width of light

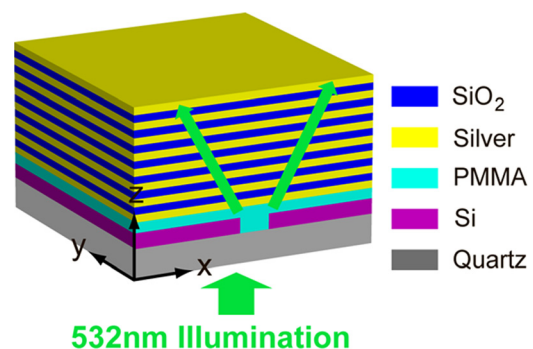


FIG. 1. Schematic of the designed ASMDL metamaterial combined with a nanoslit aperture.

^{a)}lxg@ioe.ac.cn

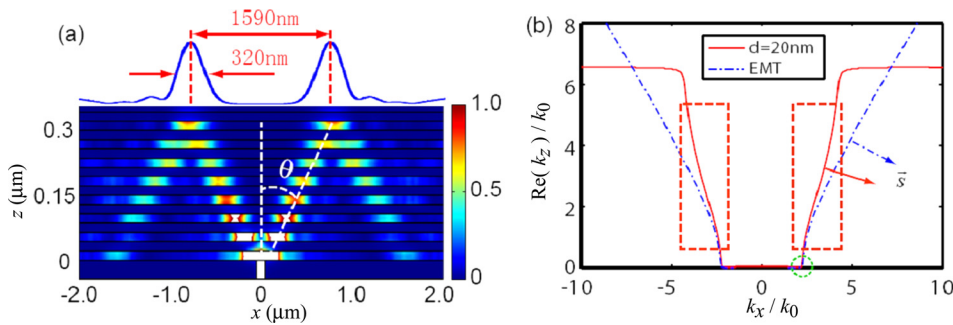


FIG. 2. (a) Simulated light distribution inside the metamaterial and (b) relationship between k_x and k_z at 532 nm for RCWA (solid line) and EMT method (dashed-dotted line), respectively.

beams. On the top Ag film, slight light energy comes out and decays exponentially in the air region. Then, the light is reflected into the metal-dielectric films. The directive propagation process can be viewed as the layer to layer coupling of SPs between the adjacent metal-dielectric-metal waveguides. So the directive propagation happens as SPs are partially coupled to the adjacent waveguide at a fixed coupling length.

Usually, it is convenient to regard the metal-dielectric systems as an effective media. The effective permittivity tensor $[\epsilon_x, \epsilon_y, \epsilon_z]$ for the anisotropic metamaterial proposed is $(-4.8270 + 0.1861i, -4.8270 + 0.1861i, 5.1985 + 0.0362i)$, leading to a hyperbolic dispersion curve of

$$(k_x^2 + k_y^2)/\epsilon_z + k_z^2/\epsilon_x = k_0^2, \quad (1)$$

opening towards x direction (dashed-dotted curve in Fig. 2(b)). We further go beyond the effective permittivity approximation and plot the effective propagation factor k_z with Bloch theory and transmission matrix (solid curve in Fig. 2(b)). For small k_x , the EMT method gives a good approximation with that by RCWA method. The two dispersion relation curves also provide one approximate way to determine the SPs propagation direction by assuming its perpendicularity to the asymptote of constant-wavelength contours as depicted in Fig. 2(b). In addition, it is worth to note that both EMT and RCWA analyses show that only evanescent waves with spatial frequency components,

$$k_x \geq \sqrt{\text{real}(\epsilon_z)}k_0 = 2.28k_0, \quad (2)$$

can propagate inside the material. This implies that the light in the propagation manner in the air is restricted and SPs light inside the ASMDL structure are not observable in the far field. For a large k_x , EMT gives nearly linear relation as the asymptote of hyperbola function. The RCWA result, however, shows the restricted k_x range for propagation modes as depicted with dashed rectangular of Fig. 2(b). The imaginary part of k_z grows quickly for k_x components outside this region, implying they are damped in the multilayer system.

The SEM picture of sample's cross section is shown in Fig. 3. The rough cross section is mainly attributed to the sample breaking off by hand and thumb before SEM operation. This issue could be improved by FIB milling or ion etching and polishing the cross section before the SEM operation. The ASMDL metamaterial fabrication process consists of the following parts. First, transparent slits with 80 nm width and $30 \mu\text{m}$ period are fabricated on silicon film with quartz substrates by shadow deposition method and then

spun with PMMA. The space between adjacent slits is large enough to avoid optical disturbance between each other. The PMMA layer is RIE etched with oxygen to get a planar profile with remained thickness of about 40 nm. Then eight layers of Ag films and seven layers of SiO_2 films were deposited alternatively with each layer thickness being about 20 nm. In the end, the top Ag layer of metamaterial is roughened by RIE (shown in the insets of Fig. 4) so that the evanescent waves associated to top surface could be scattered into far field. The silicon slits are illuminated from the substrate side with focused monochromatic laser light at wavelength of 532 nm. The sample's rough Ag surface is observed with an objective.

The picture taken by a CCD for the case of TM polarized light illumination is shown in Fig. 4(a). After directional propagating in the metamaterial, the evanescent waves form two light lines with about $1.78 \mu\text{m}$ offset on the output plane. The corresponding imaging angle θ is about 70.2° and agrees well with the simulation result of 68.2° . The measured 548 nm line width is much larger than the simulation result of 320 nm, mainly due to the scattering of evanescent waves at the rough surface (RMS 3.1 nm as shown in the inset of Fig. 4(a)) and enlarged during the far field imaging process. For the sample with a smooth top sliver surface (RMS 0.3 nm), no clear directional images could be distinguished from the picture, showing just slightly scattered light (Fig. 4(b)). As a comparison, no image is detected under TE illumination (Fig. 4(c)) because in this case no surface plasmon waves are excited and transmitted in the ASMDL metamaterial. In the control experiment without the ASMDL metamaterial, the recorded images exhibit the light diffraction pattern of the single slit with fringes appearance, which agrees with our numerical simulations plotted in the inset of Fig. 4(d).

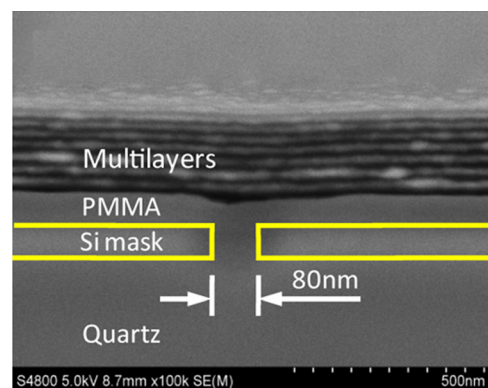


FIG. 3. SEM image of the device (cross section view).

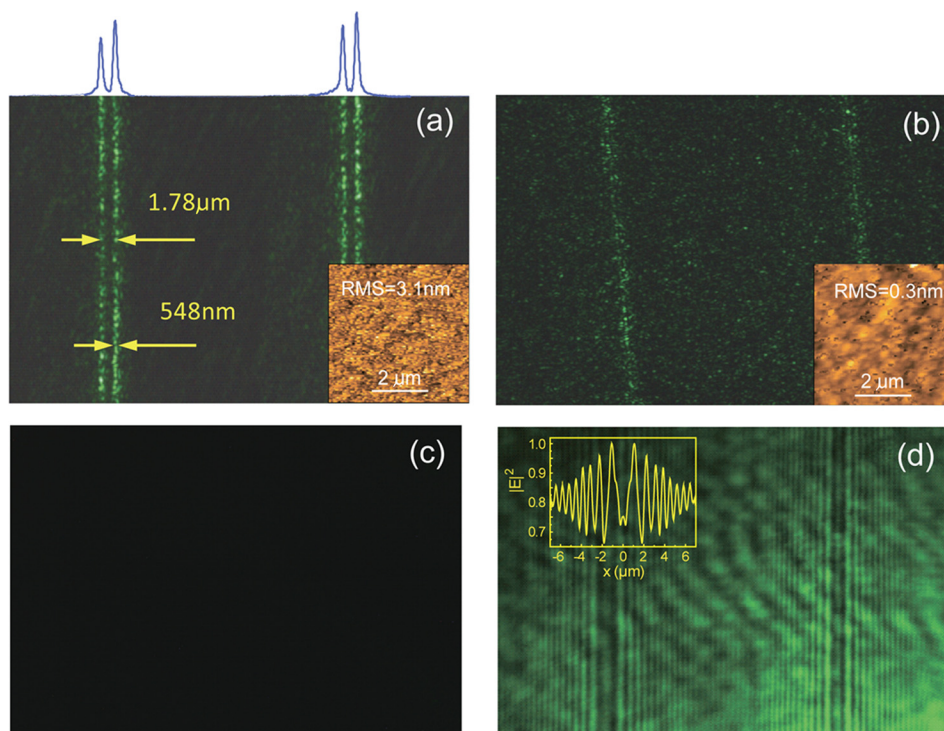


FIG. 4. Images of the ASMDL metamaterial surfaces obtained by a CCD camera. (a) and (b) are taken after and before reactive ion beam etching under TM illumination, respectively. The insets show the AFM images of top silver layer ($5 \times 5 \mu\text{m}^2$). (c) Image with rough surface and TE illumination. (d) Control experiment result without the ASMDL metamaterial. The inset shows the corresponding simulation results.

Here, to further get comprehensive understandings of directional imaging characteristics of light in the ASMDL metamaterial, its dependence on geometrical and optical parameters are presented as well. One influencing factor is the layer thickness d of Ag layer and SiO_2 layer (assuming they have equal thickness). As shown in Fig. 5 simulated by COMSOL software, the imaging angle θ increases monotonically from 62.7° to 82.0° as d increases from 5 nm to 50 nm. Intuitively, the increase of θ could be attributed to the elongated coupling length between the neighboring plasmonic waveguides at an enlarged distance. To get a quantitative idea of the thickness influence, Fig. 5 insets gives the dispersion contours between k_x and k_z for the metal and dielectric multilayers system with variant thickness d . Clearly, the effective relation between k_x and k_z deviates greatly from that defined by EMT method and shows strong dependence on layer thickness. As $|k_x|$ increases, the discrepancies of imaging directions between metamaterials at different d display more clearly. For

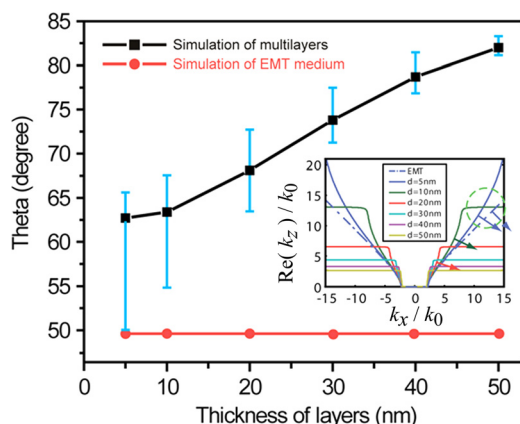


FIG. 5. The simulation result of imaging angle θ versus the thickness d of each layer.

a larger d , the steeper the dispersion relation exhibits, and results in the larger imaging angle θ . The small layer thickness d could lead to a wide range of $|k_x|$ for the evanescent waves propagation in the ASMDL metamaterial. This also implies that the light propagation does not follow a fixed direction but with some divergence (as depicted in Fig. 5 with vertical lines). The EMT theory usually delivers inaccurate imaging angle even for thickness as 5 nm, which is 49.5° and 13° smaller than that by full wave simulation. This could be understood from the inset of Fig. 5. It shows that the relation curves of k_x and k_z calculated by RCWA do not coincide well with that by EMT, especially for large k_x .

Shown in Fig. 6 is the great angle dependence of filling factor of dielectric films at a fixed 40 nm thickness period. The simulated imaging angle decreases monotonically from 77.2° to 0° as f increases from 0.125 to 0.875. This monotonic variance is in agreement with the prediction of the plasmonic coupling model, since the decrease of filled metal films indicates the easier way between the neighboring plasmonic modes and a shorter coupling length and smaller imaging angle (see Figs. 6(b) and 6(c)). It should be noted that larger filling factor of dielectric layer not only leads to small imaging angle for ASMDL metamaterials, but also delivers the low loss of SPs propagating and clear multi-reflection behaviors at two interfaces shown in Fig. 6(c).

To explain Fig. 6(a) by EMT method, one surprising point is noticed as another demonstration of EMT's limitation. The variation trend for the EMT medium agrees with the simulation results only when $f > 0.5$. For $f < 0.5$, they show totally opposite dependence on filling factor. This deviation could also be seen between the effective k_x and k_z relations calculated by EMT and RCWA, as plotted in the inset of Fig. 6(a). The RCWA curve shows specific propagation mode within a narrow k_x components range for $f=0.15$. The EMT medium curve, however, is nearly planar in this region,

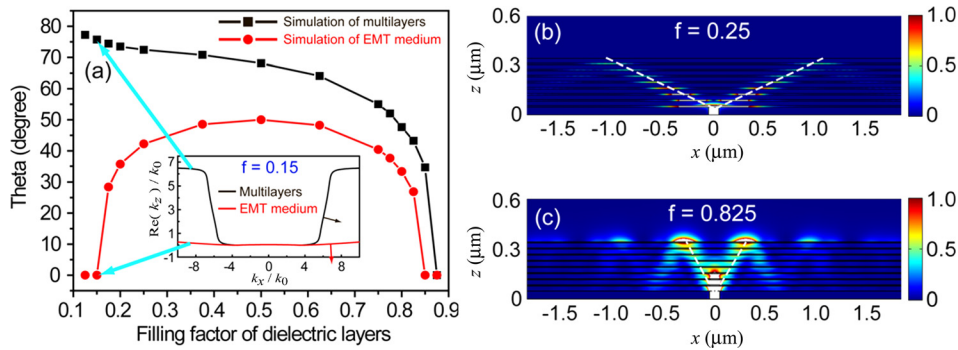


FIG. 6. The simulation result of imaging angle θ versus the filling factor f of dielectric layer. The inset demonstrates the dispersion relations with $f=0.15$. (b) and (c) are the $|E|^2$ distributions with $f=0.25$ and 0.825 , respectively.

demonstrating the failure of EMT as the approximation for strong SPs coupling in multi-layer metal-dielectric systems.

In summary, we demonstrated far field observation of directional imaging of evanescent waves in Ag/SiO₂ multilayered metamaterial by roughening the top Ag surface. The phenomenon is caused by the coupling of SPs between adjacent metal-dielectric interfaces and agrees well with numerical simulations. In addition, the geometrical parameters dependences of directional imaging behaviors are presented and demonstrating the failure of EMT method as an approximation of metal-dielectric systems for some cases. The work is believed to be helpful for designing nano-scale optical devices beyond the diffraction limit.

This work was supported by 973 Program of China (No. 2013CBA01700) and the Chinese Nature Science Grants (61138002, 61177013).

- ¹D. R. Smith and D. Schurig, *Phys. Rev. Lett.* **90**, 077405 (2003).
- ²B. Wood, J. B. Pendry, and D. P. Tsai, *Phys. Rev. B* **74**, 115116 (2006).
- ³J. B. Pendry, *Phys. Rev. Lett.* **85**(18), 3966 (2000).
- ⁴N. Fang, H. Lee, C. Sun, and X. Zhang, *Science* **308**, 534 (2005).
- ⁵R. J. Blaikie and D. O. S. Melville, *J. Opt. A, Pure Appl. Opt.* **7**, S176 (2005).
- ⁶S. A. Ramakrishna, J. B. Pendry, M. C. K. Wiltshire, and W. J. Stewart, *J. Mod. Opt.* **50**, 1419 (2003).
- ⁷C. Wang, Y. Zhao, D. Gan, C. Du, and X. Luo, *Opt. Express* **16**, 4217 (2008).
- ⁸A. Salandrino and N. Engheta, *Phys. Rev. B* **74**, 075103 (2006).
- ⁹Y. Xiong, Z. Liu, and X. Zhang, *Appl. Phys. Lett.* **94**, 203108 (2009).
- ¹⁰W. Wang, H. Xing, L. Fang, Y. Liu, J. Ma, L. Lin, C. Wang, and X. Luo, *Opt. Express* **16**, 21142 (2008).
- ¹¹P. A. Belov and Y. Hao, *Phys. Rev. B* **73**, 113110 (2006).
- ¹²B. Zeng, X. Yang, C. Wang, Q. Feng, and X. Luo, *J. Opt.* **12**, 035104 (2010).
- ¹³P. B. Johnson and R. W. Christy, *Phys. Rev. B* **6**, 4370 (1972).
- ¹⁴E. D. Palik, *Handbook of Optical Constants* (Academic Press, 1998).